Fall 12-15-2018

A Novel Splitting Beam Laser Extensometer Technique for Kolsky Tension Bar Systems

Colin Loeffler
Southern Methodist University, cloeffler@smu.edu

A NOVEL SPLITTING BEAM LASER EXTENSOMETER

TECHNIQUE FOR KOLSKY TENSION

BAR SYSTEMS

Approved by:

_____
Dr. Xu Nie
Assistant Professor

_____
Dr. Xin-Lin Gao
Professor

_____
Dr. Wei Tong
Professor

A NOVEL SPLITTING BEAM LASER EXTENSOMETER TECHNIQUE FOR KOLSKY TENSION BAR SYSTEMS

A Thesis Presented to the Graduate Faculty of

Lyle School of Engineering

Southern Methodist University

in

Partial Fulfillment of the Requirements

for the degree of

Master of Science in Mechanical Engineering

by

Colin Loeffler

B.S., Mechanical and Energy Engineering, University of North Texas

December 15, 2018

Loeffler, Colin B.S. University of North Texas, 2014

A Novel Splitting Beam Laser Extensometer Technique for Kolsky Tension Bar Systems

Advisor: Professor Xu Nie

Master of Science in Mechanical Engineering Conferred December 15, 2018

Thesis completed August 20, 2018

The Kolsky (Split Hopkinson) Bar has become a well-known and established experimental technique for characterizing the mechanical behavior of materials subjected to dynamic loading conditions. Kolsky bar based experimental techniques facilitate the application of controlled and repeatable dynamic loading conditions to a specimen as well as the high resolution measurement of the resulting mechanical response. In recent decades the technique has been refined and adapted to provide more complex dynamic stress-states beyond uniaxial compression. However, the increasing complexity of the experimental apparatus introduces uncertainty to the traditional specimen deformation measurement techniques.

In this thesis, a direct non-contact optical measurement technique is introduced to significantly improve the resolution of specimen deformation measurements. This novel technique, known as a splitting beam laser occlusive extensometer, is capable of measuring the displacement of both specimen ends with independent and tunable resolutions. This technique provides specimen deformation measurements with accuracy and precision superior to that of traditional methods used in Kolsky bar experiments. The relatively low cost and simplicity of this system make it a desirable alternative to other non-contact direct measurement techniques.

The proposed technique is then further expanded upon with the addition of a third measurement channel. The third channel is specifically introduced to measure the small displacements characteristic of a material undergoing elastic deformation, without sacrificing the measurement range required to capture the relatively large plastic deformations observed in ductile materials

The proposed techniques are demonstrated and validated using dynamic tensile test of common metallic materials with well-known properties. Additionally, these experimental results are used to investigate the accuracy of traditional deformation measurement techniques used in Kolsky tension bar experiments.

TABLE OF CONTENTS

LIST OF FIGURES

LIST OF TABLES

Table Page

NOMENCLATURE

A	Cross sectional area of the specimen
A_B	Bar cross-sectional area
A_s	Specimen cross -sectional area
C'	Fraction of the total elastic deformation that occurs in the specimen gage section.
C_B	Elastic wave speed in the bar material
δ_I	Displacement of the Incident bar end
δ_T	Displacement of the Transmission bar end
ΔL_s	Total specimen deformation
ΔL_g	Total deformation in the gage section of the specimen
ΔL_t	Total deformation in the transitional sections of the specimen
E_B	Young's Modulus of the Bar Material
E_s	Young's Modulus of the specimen material
$\dot{\varepsilon}$	Specimen Strain-Rate
ε_R	Reflected strain wave
ε_T	Transmitted strain wave
$\varepsilon_{laser-elastic}$	Elastic specimen strain measured by the 3 channel laser extensometer
$\varepsilon_{laser-total}$	Total strain measured by the by the 3 channel laser extensometer
ε_t	Axial strain in the transitional portion of the specimen
ε	Specimen strain
F	Total axial force applied to the specimen
κ_1	Laser sensitivity coefficient for detector 1

κ_2	Laser sensitivity coefficient for detector 2
κ_3	Laser sensitivity coefficient for detector 3
L_s	Specimen length
r_0	Radius of the specimen gage section
R	Radius of the specimen shoulder
r	Specimen radius
σ_T	Transmitted stress wave
σ	Specimen Stress
u_1	Detector 1 output voltage
u_2	Detector 2 output voltage
u_3	Detector 3 output voltage
x	Axial location in the specimen transitional section

ACKNOWLEDGEMENTS

I would like to express the utmost gratitude to my academic advisor Dr. Xu Nie for providing the knowledge and guidance that facilitated this work and many of my other academic pursuits. I must also acknowledge Dr. Ying Qui who spent many hours in the lab working to perfect these experimental techniques. Without her hard work and dedication, the accomplishments presented here would not have been possible. Additionally, I'd like to thank Dr. Bo Song for his technical expertise and support. Working with such esteemed colleagues and mentors has provided me with invaluable knowledge and experience. Last but not least, I must thank my wife and family for the endless support and motivation.

Chapter 1

INTRODUCTION

1.1. **Dynamic Testing Techniques**

The tensile properties of materials are important for the assessment of material performance, development and calibration of predictive material models, as well as failure and fracture analyses in engineering applications. Standard testing procedures and hardware used for measuring the mechanical response of materials under low-rate tensile loading have been well established. However, many challenges arise when measuring the behavior of materials under high strain-rate tensile loading conditions due to limitations of the experimental apparatus, procedure, and diagnostic techniques [1].

1.1.1. Dynamic Compression

Dynamic mechanical properties of soft materials were first reported by Taylor in 1946 [2,3]. Later, high strain-rate compression experiments on rubbers, plastics and metals were conducted using an apparatus known as the Kolsky bar, which used a detonator to generate stress waves in an elastic rod to dynamically load a specimen. Figure 1 shows a schematic of the first Kolsky bar system introduced in 1949 [4].

Over the decades following it's invention, the Kolsky Bar technique was implemented to characterize the dynamic behavior of a wide variety of materials including metals [5–8], ceramics [9–11], concrete [12–14], polymers [15–17], biomaterials [18–20], etc. The experimental technique has been extensively improved as well as adapted to provide various stress states [21–32]. The Kolsky Compression bar is now a well-established and widely accepted method of applying controlled dynamic loading conditions to a material and measuring the resulting mechanical response.

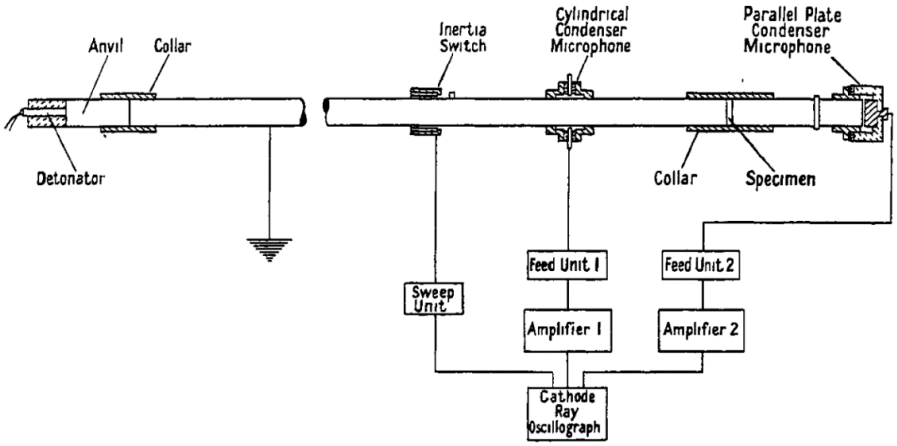

Figure 1.1 A schematic of the original Kolsky Bar apparatus [4]

The standard Kolsky Compression Bar consists of two long elastic rods aligned along a common axis and placed end to end, the specimen of interest is then placed between the two bars. A striker bar is then accelerated to impact the opposite end of the first bar, known as the incident bar, this impact generates a compressive stress wave that propagates along the length of the Incident Bar towards the Specimen. Upon reaching the specimen, a portion of this wave is reflected back up the Incident bar, while the remainder is transmitted through the specimen and into the second bar, known as the transmission bar. A schematic of the typical Kolsky Compression Bar is shown in Figure1.2. The stress waves travelling along the bars can be measured and recorded using strain gages attached to the bar surface.

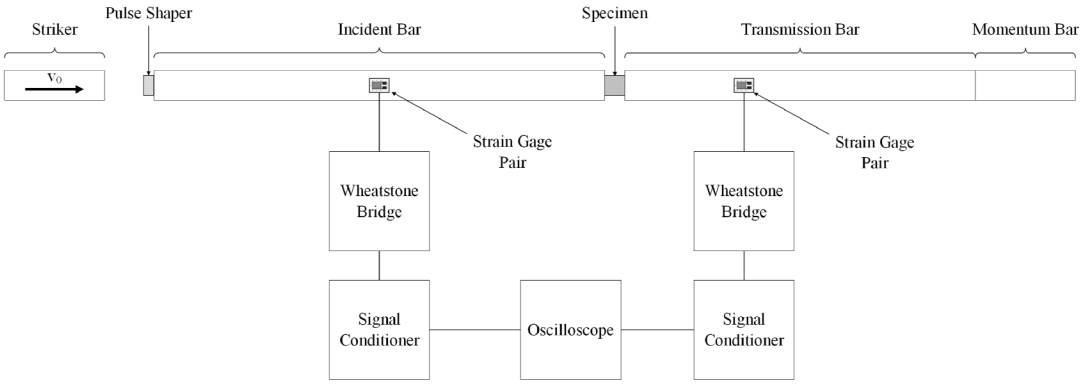

Figure 1.2 A Schematic of a typical Kolsky Compression Bar

Assuming the stress waves are one dimensional and propagate along the bars without dispersion, the stress and deformation history of the specimen can be calculated using the recorded waves [21]. The specimen engineering-stress history is proportional to the Transmitted stress wave and can be calculated using Equation (1.1).

$$\sigma = \frac{A_B}{A_s}\sigma_T = \frac{A_B}{A_s}E_B\varepsilon_T \tag{1.1}$$

The transmitted stress, σ_T is taken to be the transmitted strain wave ε_T multiplied by the Elastic modulus of the bar material represented by E_B. The cross-sectional areas of the bars and specimens are represented by A_B and A_S respectively. The engineering strain-rate of the specimen is directly proportional to the reflected strain wave as described by Equation (1.2).

$$\dot{\varepsilon} = -2\frac{C_B}{L_s}\varepsilon_R \tag{1.2}$$

Where, ε_R is the reflected strain wave, C_B is the elastic wave speed in the bar material and, L_s is the specimen length. Finally, the specimen engineering-strain history is obtained by integrating the strain-rate according to Equation (1.3).

$$\varepsilon = -2\frac{C_B}{L_s}\int_0^t \varepsilon_R\, dt \tag{1.3}$$

It should be noted that equations 1.1-1.3 use the engineering stress and strain formulation which will be used hence forth in this report. The specimen stress and strain histories are a function of both the applied loading conditions as well as the constitutive behavior of the material. In a traditional quasi-static material testing machine, the loading conditions are continuously adjusted using a feed-back control loop. Due to the High rate of loading this type of control is impossible, therefore the Kolsky Bar is an open loop system. This means that the profile of the input or incident stress wave must be tailored to the constitutive behavior of the specimen to achieve the desired loading conditions e.g. constant strain-rate deformation. The profile of the

incident wave can be adjusted through a process known as “pulse shaping”. There are various pulse shaping methods that can be used to achieve the desired loading wave, however the most common involves placing a soft tip material often called a “pulse shaper” between the incident bar and striker. As the striker impacts this tip material, the large plastic deformations of the tip material alter the profile of the stress wave transferred into the incident bar. In addition to changing the profile of the incident wave, the pulse shaper also acts as a mechanical low-pass filter, reducing high frequency oscillations in the loading wave which reduces wave dispersion [21,33]. The Kolsky compression bar is widely used, thanks in part to its relative simplicity, however extending this technique to apply different dynamic stress states e.g. Tension, Torsion, Tri-Axial compression, etc. Requires more complicated mechanisms that introduce additional challenges.

1.1.2. Development of the Kolsky Tension Bar

Harding et al. [28] were the first to obtain tensile stress-strain curves of aluminum alloy and molybdenum at high strain rates in 1960. Hauser and Harding et al. [29,30] designed a tension bar system riding inside a hollow tube, with one end of the tube joined to the “loading end” of the solid incident bar. A Compressive stress wave was generated by impacting the opposite end of the tube, this wave would then propagate down the length of the tube until reaching the joint where it would be transmitted into the incident bar as a tensile stress wave. In the same year, Lindholm et al. [27] achieved dynamic tensile loading using a conventional Kolsky Compression Bar by modifying the specimen geometry to a special “Top Hat” design. In 1981 Nicholas [31] revised the specimen section of a compression bar setup to accommodate a tensile specimen, and then placed a rigid collar surrounding the specimen gage section. The collar was initially in contact with both the incident and transmission bars to prevent the specimen from being compressed while the compressive wave traveled across the gage section. When the compressive wave was reflected from the free end of the transmission bar as a tensile wave, the specimen was loaded in tension and the collar was disengaged from the bars. In 2009 Owens et al. [24] achieved dynamic tensile loading through the use of a hollow striker tube which could be slid along the surface of the incident bar and accelerated to impact a flange rigidly connected to the bar’s end generating a tensile stress wave in the incident bar.

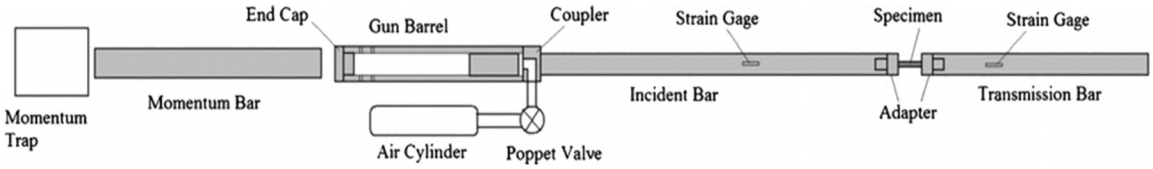

Figure 1.3 A schematic of the Kolsky Tension Bar
proposed by Song et al. [23]

In 2011 Song and Guzman proposed a similar system that utilized a hollow "Incident Tube" rigidly connected to the solid incident bar on one end and capped at the opposite end [23,34]. This arrangement facilitates the use of a solid striker bar which is accelerated inside of the incident tube to impact the capped end of the tube. This impact generates a tensile stress wave that propagates down the tube and into the incident bar. The major advantage of this configuration is the ability to use the same pulse shaping technique that was developed for Kolsky Compression Bar systems in dynamic tension experiments due to the use of the same striker geometry.

1.2. **Specimen Strain Measurement during High Strain-Rate Experiments**

Unlike free contact between the specimen and the bar ends in a Kolsky compression bar experiment, in a Kolsky Tension Bar experiment the tensile specimen needs to be properly attached to the bar ends in order to transmit tensile stress into the specimen without introducing unwanted damage or deformation. A common method of specimen attachment involves machining threads into the bar ends so that cylindrical specimens with matching threads on either end can be screwed directly into the bars. However, this method introduces potential uncertainties in the calculation of specimen strain using the wave propagation theory (outlined in section 1.1.1). For example, the threaded connection at the bar/specimen interface introduces many free surfaces in the wave path which may disrupt stress wave propagation. As a result, the reflected wave recorded by the strain gages may not yield an accurate specimen strain measurement, particularly at small strains (less than 1%) [35]. Li et al. [36] estimated the strain error induced by the threaded connection between the specimen and bars. In 1997 Nguyen et al. noted that the spurious waves generated at the end surface between the threaded specimen and input bar were responsible for the imperfect incident compressive pulse transmitted through the collar in high-strain rate tensile experiments. Two decades later Nguyen at al. [37]

studied the effects of thread shape on the wave propagation characteristics of a calibration specimen and used these results to propose a thread shape design guide to maximize accuracy in dynamic tension experiments. Moore et al. [38] studied the stress-wave propagation in a Kolsky Bar system with a threaded interface and proposed a primary-pulse model to improve the accuracy of material property calculation. Song et al. [35] attempted to mitigate the effects of the threaded interface mechanically with the addition of lock-nuts to pre tighten the threaded connection thereby improving the thread contact. Their results showed that the application of locknuts minimized the pseudo stress peaks caused by the threaded connection, however the effect of locknuts on specimen strain measurement, particularly at small strains, has not been fully investigated yet.

Due to the uncertainty caused by the threaded connection necessary for tensile testing, an additional strain measurement method is needed to directly measure the specimen strain. High-speed digital image correlation (DIC) has been extensively used for direct full-field specimen strain measurements over a wide range of loading rates. The DIC technique requires the application of a random speckle pattern on to the specimen surface, allowing a motion tracking algorithm to measure the displacement of each speckle and therefore calculate the displacement/strain field on the specimen surface. A similar technique known as the grid method uses a regular grid as opposed to a random speckle pattern to measure small displacement and strain components on the specimen surface. The accuracy of these full field measurement techniques largely depends on the quality of the imaging system and processing algorithms. While these techniques are capable of providing the spatial and temporal resolution required for dynamic materials characterization [39–42], the sophisticated equipment required often makes these techniques cost prohibitive.

In addition to the full-field measurement methods mentioned above, laser-based strain measurement techniques have been widely published in the literature [35,43–48]. Zhu et al. [43,44] designed a high-speed laser extensometer, based on laser interferometry, to measure the tensile strain history at moderate strain rates up to 24 s^{-1}. Li and Ramesh [45] developed an optical-based direct non-contact extensometer technique for radial deformation measurement, and their results agreed with the measurements made by strain gages placed directly on the specimen. Guzman et al. [34] adopted a single channel laser extensometer system to measure large tensile strains at high strain rates, while Joyce et al. [47] used the single channel laser extensometer to measure the compressive strain of silicone samples and obtained accurate axial strain measurements at

different strain rates. They also noted that the measurement accuracy was deteriorated by the large radial expansion of the soft material at high axial strains. Song et al. [35] and Nie et al. [46] further expanded this technique to a two-channel system to independently track the displacement of both specimen ends. A similar two-channel laser extensometer apparatus was used by Panowicz et al. [48] to test two different specimen materials (5251 aluminum and OFE copper) and two different bar materials (aluminum alloy Al7075-T6 and maraging steel grade MS350) at various high strain rates, which further verified the capability of the laser extensometer. However, none of these laser extensometer systems are capable of simultaneously measuring both small and large strains with high resolution. The novelty of the laser extensometer presented in this study is the addition of a third channel to facilitate the precise measurement of small displacements at high strain rates, which provides a more accurate measurement of dynamic material properties, particularly at small strains.

1.3. **Outline of Research Objectives**

This thesis consists of four chapters organized as follows: Chapter one provides back ground on the Kolsky bar technique, a literature review of Kolsky tension bar techniques, and a brief summary of strain measurement methods used for high rate deformation experiments.

Chapter two outlines the motivation for and construction of a novel splitting-beam laser extensometer designed for use in Kolsky tension bar experiments. A modified laser occlusive extensometer technique was developed to measure the specimen strain with reasonably high and tunable resolutions in Kolsky tension bar experiments. This technique uses the novel concept of splitting a single laser beam into two independent sections to track the displacement histories of the incident and transmission bar ends separately with independent resolutions. This technique ensures precise small strain measurements without sacrificing the range required for large strain measurement. In addition, this technique minimizes the uncertainty caused by rigid body motion of the specimen, which is a result of slight variation in laser intensity along the gage length. Dynamic tensile tests of Vascomax® maraging C250 alloy were then used to validate the technique. These experiments demonstrated that the new technique was capable of accurate strain measurement in Kolsky tension bar experiments up to the peak tensile strength of the material.

Chapter three introduces an improved three-channel splitting-beam laser extensometer with dual resolution. The added higher resolution channel facilitates dynamic elastic strain measurements with higher fidelity and minimal uncertainties. By adopting a dual-channel configuration on the incident bar side, the resolution and measurement range of this laser extensometer were coordinated between the two channels to provide highly precise measurement at both small and large strains under high strain-rate loading conditions. With this novel design, a maximum resolution of approximately 500 nm can be obtained for the specimen displacement measurement, which corresponds to a strain of 0.0079% for a specimen with a 6.35-mm gage length. To further improve measurement accuracy, a pair of lock nuts were used to tighten the tensile specimen to the bars in an effort not only to prevent the specimen from potential deformation and damage during installation but also to provide better thread engagement between the specimen and the bar ends. As a demonstration of this technique, the dynamic tensile stress-strain response of a 304L stainless steel was characterized with high resolution in both elastic and plastic deformations.

Chapter Four summarizes the main findings and conclusions of this study and proposes some future work on the application of this new laser extensometer technique.

Chapter 2

A NOVEL SPLITTING-BEAM LASER EXTENSOMETER TECHNIQUE FOR KOLSKY BAR

2.1. **Introduction**

Kolsky bars, also known as split Hopkinson bars, have been extensively employed to characterize the dynamic stress-strain response of materials [4]. In Kolsky bar experiments, the measurement of specimen strain is more challenging than the measurement of specimen stress, particularly when the specimen strain is small. Conventionally, specimen strain in Kolsky Bar experiments is calculated using the reflected wave [4]. However, there are many cases in which this method may not provide an accurate measurement of specimen strain. For example, in uniaxial tension experiments, the complex interfacial conditions at the connection between specimen and bars may disrupt the wave propagation, introducing error to the strain calculation. Therefore, non-contact optical methods for direct specimen strain measurement have been developed in lieu of the conventional strain measurement technique.

The laser extensometer has become a straight forward method of non-contact measurement of specimen strain in Kolsky bar experiments. This technique utilizes a uniform laser sheet which is projected across the specimen's gage section, parallel to the axis of deformation. When the specimen is deformed, the change in the gage length of the specimen results in a change in the amount of light that can pass between the bar ends. This change can then be converted to a voltage signal by a high-frequency-response laser detector located behind the specimen [49,50]. With proper calibration, the specimen gage length can be measured throughout the deformation process, and therefore the specimen strain history can be directly measured. Satisfactory results were reported by Li et al. using this technique to measure the dynamic tensile behavior of several metallic alloys and composites with a Kolsky tension bar system [45]. Within the last decade, this method has been implemented to a small-diameter Kolsky tension bar system for dynamic tensile testing of single fibers [51,52].

In Kolsky Bar experiments both the incident and transmission bar move in the same direction but at different velocities. This relative velocity difference results in the specimen strain, but there is also rigid body motion superimposed with the absolute deformation of the specimen. If there is a slight variation of laser intensity along the measurement gage section, which is often the case in real experiments, the rigid body motion will cause a small output signal superimposed on the specimen deformation signal. If the specimen strain is small, this error caused by rigid body motion coupled with non-uniform laser intensity may be significant. Calibration of the laser extensometer is performed using a high-resolution differential translation stage to precisely adjust the gage-section gap. Using the translation stage, the gap is reduced by increments of 10μm and the corresponding change in laser-detector output voltage is recorded. By repeating this procedure, several times, a relationship between the gap size and output voltage can be developed. In order to demonstrate the variation in the laser intensity, this calibration procedure was repeated over a small displacement range (~200μm) at three locations along the measurement gage section approximately 300μm apart. Figure 2.1 summarizes the results of these calibrations with a plot of output voltage as a function of gap size. The results show a linear relationship between output voltage and gap size at all locations across the measurement gage section. However, the slope of this linear correlation changes at each of the three locations, this is due to the slight variation in laser intensity across the measurement gage section.

In addition to the error introduced by the rigid body displacement of the specimen, the measurement resolution is limited due to the relatively large gage section used in Kolsky tension bar experiments. Song et al. showed that this resolution can be improved by tracking the displacement of the incident-bar/specimen interface separately, however the 100μm resolution achieved using this technique was still not sufficient to measure the small strains observed during the elastic deformation of the material being studied [1].

In this study, the single laser beam of a conventional laser extensometer is split into two so that the displacement of the incident and transmission bar ends can be measured independently. This arrangement allows the motion of the two bar ends to be measured with independent and tunable resolutions. Additionally, the error introduced by the variation of laser intensity will be reduced because the local laser sensitivities at each bar end will be calibrated separately. As a demonstration, this new splitting-beam laser extensometer was coupled with a Kolsky tension bar to characterize the dynamic tensile stress-strain response of a VascoMax® maraging C250 steel alloy.

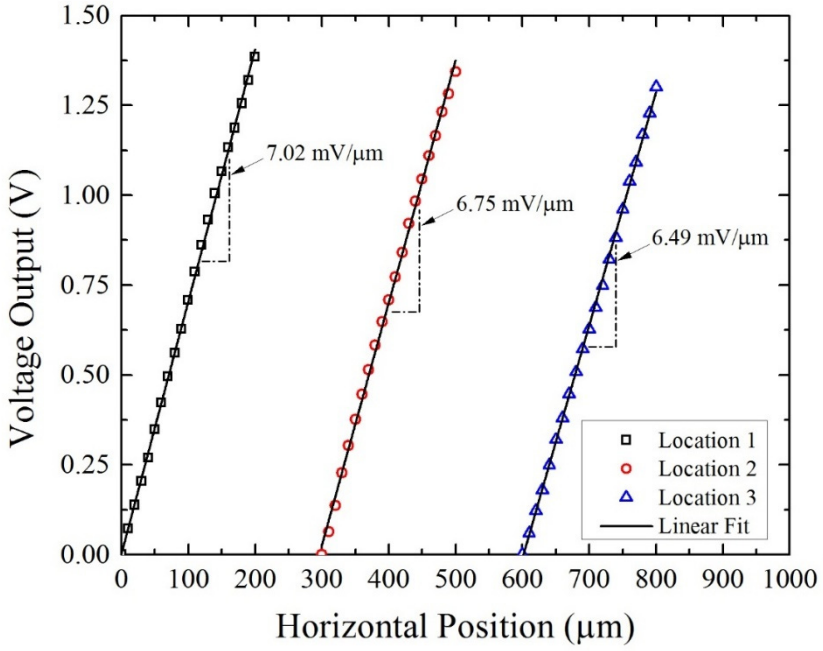

Figure 2.1: Results of laser sensitivity calibration preformed at three separate locations along the measurement gage section, the slight variation in slope at each location is a result of the non-uniform laser intensity.

2.2. **Experiments**

2.2.1. The Kolsky Tension Bar

The Kolsky tension bar used in this study, shown in Figure 2(a), utilizes the design proposed by Song et al. [23] and Guzman et al. [34]. This innovative design utilizes a solid cylindrical striker bar that slides inside a hollow gun barrel. The gun barrel is plugged on one end and rigidly connected to the incident bar at the opposite end. Compressed gas is then used to accelerate the striker bar inside of the gun barrel away from the incident bar to impact the plugged end of the barrel. This impact generates a tensile stress wave in the gun barrel that propagates down its length and into the incident bar. This design uses the same striker bar geometry as Kolsky compression systems, which allows the direct implementation of the pulse shaping technique discussed previously to dynamic tension experiments. This convenient pulse shaping technique allows tailoring of the incident wave to facilitate constant strain rate deformation and dynamic stress equilibrium in the specimen. In this study, a rubber disk of 5.56mm in diameter and 0.82mm thick was placed on the inside surface of the impact plug to serve as the pulse shaper for the Maraging steel specimens.

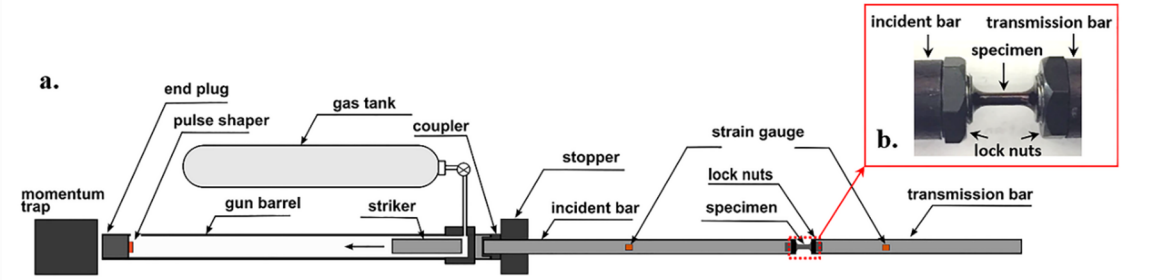

Figure 2.2: (a) A Schematic of the Kolsky Tension Bar system and (b) a typical specimen installed in the bars with lock nuts.

The Geometry of the Maraging steel specimens used in this study is shown in Figure 2.3. The gage section, over which measurements were made, was 6.35mm in length and 3.18mm in diameter. The transitional sections of the specimens, between the gage section and threads, were designed to reduce undesired stress concentrations and ensure that failure occurred in the gage section. The red line in Figure 2.3 represents the gap, over the gage section and transitional sections of the specimen, through which the laser extensometer passes. Also shown in figure 3 are the ½-20 UNF-2A threads machined on both ends of the specimen. These threads allow the specimen to be directly threaded into the matching threads in the Incident and transmission bar ends. Additionally, a pair of 4.78mm thick ½-20 UNF-2B lock nuts were placed on the specimens before being inserted into the bars as shown in Figure 2.2(a). These lock nuts were then pre-tightened against the bar ends to ensure good thread engagement. This simple and effective method eliminates the need for any thread sealant like Teflon tape or thread locker. However, care must be taken when tightening the locknuts to avoid applying any torque to the specimen gage section which could cause premature damage or failure. The effect of the locknut torque level on the experimental results will be investigated in a later section.

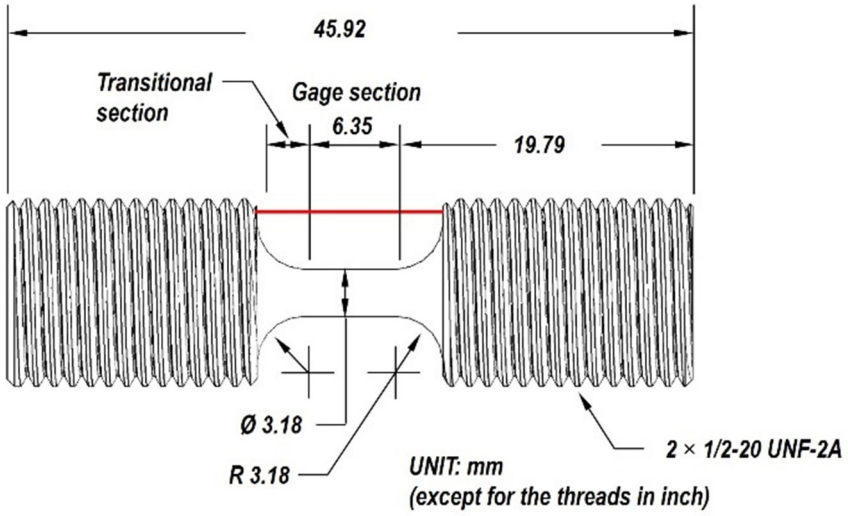

Figure 2.3: Geometry of the VascoMax® maraging C250 steel tensile specimens

2.2.2. The Two-Channel Splitting Beam Laser Extensometer

The basic arrangement of the splitting beam laser extensometer is shown in Figure 2.4. A 50mW line laser is passed through a plano-convex spherical lens to generate a collimated sheet laser perpendicular to the bars. This laser sheet is projected towards the gap between the bar ends such that a portion of the beam passes through the gap while the remainder is blocked by the bars. The portion of the beam that passes through the gap is then divided into two independent sections by a right-angle prism mirror. The apex of the right-angle mirror serves as a stationary reference line, allowing the motion of each bar end to be tracked independently. In addition to facilitating the independent tracking of each bar end, this design prevents any possible interference between the two laser detectors. After being separated, the two laser beams are each passed through a spherical lens and directed into two laser detectors. The laser detectors used (Thorlabs PDA 36A) have tunable resolutions with a correlated frequency response. At the bandwidth of 100 kHz or higher that is usually required for Kolsky bar experiments [21], the laser detector is capable of measuring the displacement with a resolution of approximately 100 nm, which corresponds to a strain resolution of 0.0016% for a specimen 6.35-mm long. The use of two independent laser detectors allows the resolution and bandwidth for the Incident and Transmission bar end displacement sensors to be selected independently. In Kolsky bar experiments the transmission bar end moves at a lower velocity than the incident bar, this difference in velocities is a result of the specimen strain. This also means that the total displacement of the transmission

bar will be smaller than that of the incident bar and therefore the resolution of the transmission bar displacement sensor should be higher.

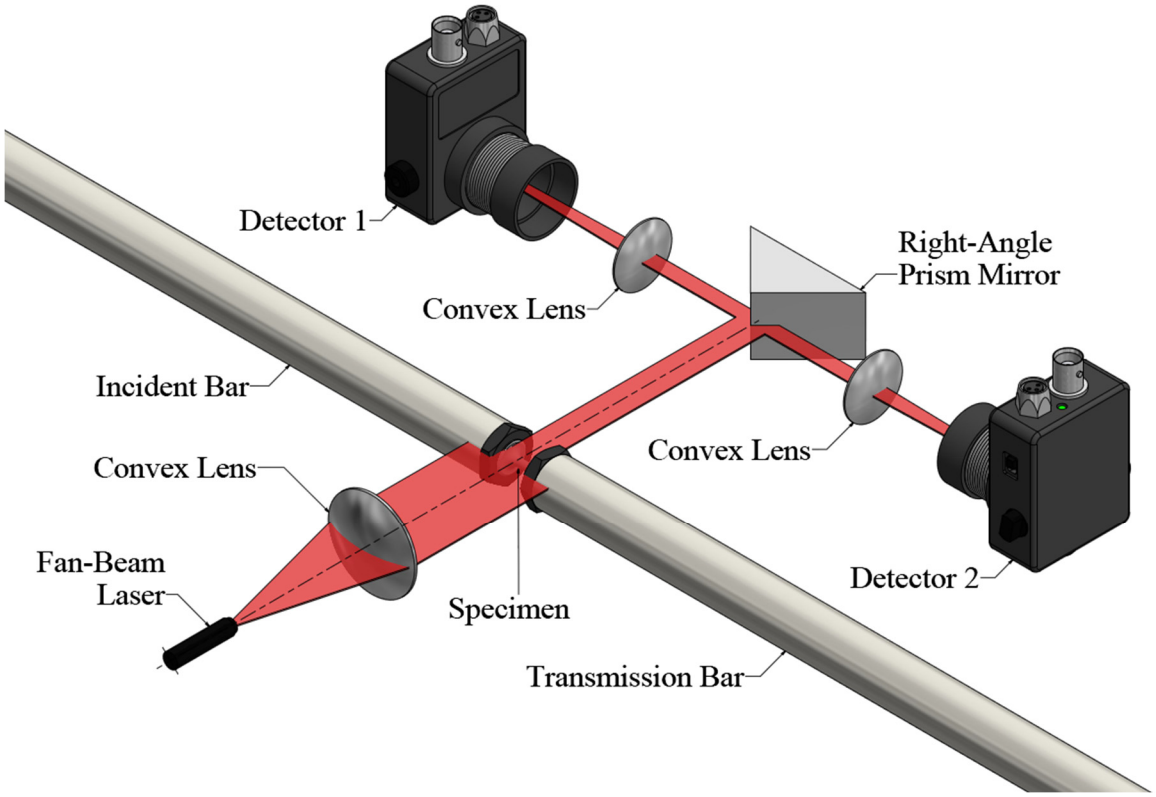

Figure 2.4: A 3D model of the splitting beam laser extensometer for Kolsky bars.

The new dynamic splitting-beam laser extensometer was applied to Kolsky tension bar experiments on an ATI Vascomax® maraging C250 alloy. The raw material was normalized at 927°C for one hour followed by water quenching and annealing at 816°C for one hour before rapid air cooling. After machining, the tensile specimens were tempered at 482°C for three hours and then air cooled. The specimens prepared for dynamic tension experiments were machined into cylindrical dog bone specimens of the geometry shown in figure 2.3 with a diameter of 3.18mm and a gage length of 6.35mm. The Kolsky tension bar used in this study was of the design described previously [1,34]. The 19.05-mm diameter incident and transmission bars made of Vascomax® maraging C350 alloy were 3658- and 2134-mm long, respectively. Both incident and transmission bars had ½-20 UNF-2B threads machined into the specimen ends so that the tensile specimens could be directly threaded into the bar ends without the need of adapters.

2.2.3. Measurement of High-Rate Stress-Strain Response

A set of signals from a typical dynamic tensile experiment, as recorded by the oscilloscope, are shown in Figure 2.5. These signals include the strain recorded in both the incident and transmission bars, the displacement of the bar ends measured by the laser extensometer, and the specimen strain measured by a strain gage attached directly to the specimen surface. As shown in Figure 2.5, the strain gage failed shortly after the dynamic load was applied, however the data recorded will serve to compare the small strain (<2%) performance of the laser extensometer. It must be noted that the specimen strain gage precisely recorded the specimen deformation within the area covered by the strain gage, while the splitting-beam laser extensometer measured the total deformation of both gage and transitional (non-gage) sections of the specimen. In order to calculate the strain of the gage section alone using the laser extensometer data, a correction procedure described in Ref. [1,35] and outlined in section 3.2.2, has been employed to compensate for the excess deformation in the transitional sections of the specimen.

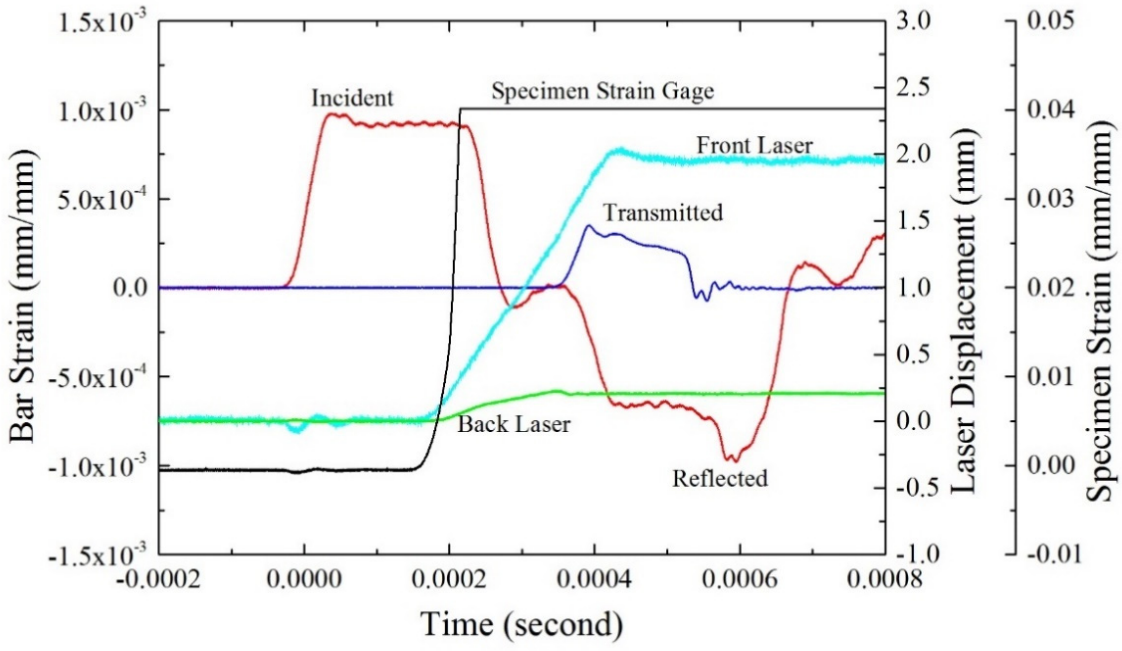

Figure 2.5: The strain signals from various sources directly recorded with an oscilloscope during a Kolsky tension bar validation test.

The stress strain curve obtained using the corrected laser extensometer data is compared with the curve obtained by the direct strain gage measurement in Figure 2.6. It must be noted that the strain directly measured by the strain gage is only valid up to approximately 2%. Figure 2.6 clearly shows good agreement between the mechanical behavior measured by the strain gage and laser extensometer in the elastic deformation region. However, after the specimen reaches a peak stress of 2.5GPa the two strain measurements begin to deviate from one another significantly, this is due to the strain gage exceeding its operating limits. This deviation could also be caused by the correction applied to the laser extensometer data, which is based on the assumption of perfect plasticity in the specimen gage section [1] which is not a valid assumption for the Vascomax® maraging C250 alloy being investigated. The stress-strain curve shown in figure 2.6 suggests that this material may exhibit early-onset localized plastic-deformation, such as necking, which would result in an erroneous calculation of the plastic strain in the gage section using the correction procedure. Nevertheless, the capability of this technique to measure the small strain deformation of specimens under dynamic loading conditions has been demonstrated in addition to its ability to capture the complete specimen deformation history.

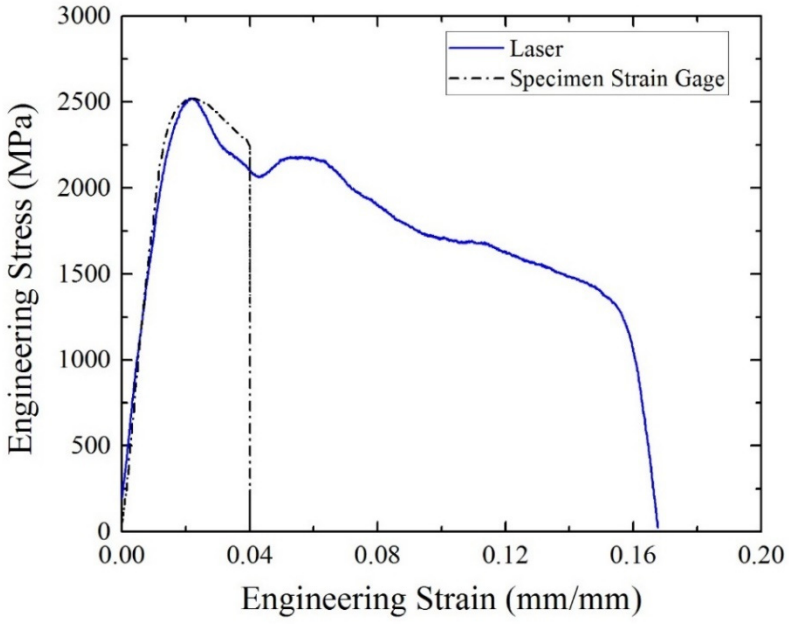

Figure 2.6: The stress strain curves for a single specimen obtained using the splitting-beam laser extensometer and direct strain gage measurement.

2.3. **Conclusion**

A conventional laser occlusive extensometer was modified for use with Kolsky bar experiments by taking the innovative approach of splitting the laser beam into two different channels. This novel design is capable of tracking both bar/specimen interfaces independently, which allows the resolution of each detector to be tuned separately to optimize the accuracy of specimen strain measurements. This design facilitates measurement of the small- and large-strain deformation of the specimen with high resolutions and bandwidths. A dynamic tension test of a Vascomax® maraging C250 alloy specimen was conducted on a Kolsky tension bar as a validation test. The results showed that the elastic portion of the dynamic tensile stress-strain curve measured with the splitting-beam laser extensometer technique agreed well with the direct specimen strain gage measurement. The validation test demonstrated the capability of this technique to measure both small and large specimen deformations

Chapter 3

IMPROVED EXPERIMENTAL AND DIAGNOSTIC TECHNIQUES FOR DYNAMIC TENSILE STRESS-STRAIN MEASUREMENT WITH A KOLSKY TENSION BAR

3.1. **Introduction**

While Kolsky tension bar techniques have been improved to increase the accuracy and precision of dynamic material characterization, challenges associated with specimen gripping, short specimen gage-section, and geometric discontinuities still compromise the accuracy of conventional strain measurement techniques in Kolsky tension bar experiments. In this chapter, a novel three-channel laser extensometer with hierarchical resolution was developed to directly track the displacements at each shoulder of the tensile specimen, with the goal of measuring both small and large-scale deformations with high resolution. Figure 3.1 shows a 3D illustration of the three-channel laser extensometer which has been directly adapted from the two-channel system presented in Chapter 2. By adopting a dual-channel configuration on the incident bar side, the resolution and measurement range of this laser extensometer were coordinated between the two channels to provide precise measurement of both small and large strains during high strain-rate loading. On the transmission bar side an amplified channel, similar to that used on the incident bar side, was adopted to measure the smaller transmission bar displacement with high resolution. With this novel design, a maximum displacement resolution of approximately 500 nm can be achieved while maintaining a sufficient measurement range, which corresponds to a strain resolution of 0.0079% for a specimen with 6.35-mm gage length. To further improve the material characterization accuracy, a pair of locknuts were used to pre-tighten the specimen/bar interface in order to ensure good thread engagement. Comparative studies were conducted on 304L stainless steel specimens without locknuts, with lock nuts tightened to 7.8 N·m, and with lock nuts tightened to 15.6 N·m. The correction method proposed by Song et al. [35] was applied to the strain data measured by the laser extensometer to account for the additional strain contributed by the transitional

(shoulder) of the specimen. The dynamic Young's modulus of 304L stainless steel was then determined from the corrected stress-strain curves and compared with the quasi-static value to demonstrate the effectiveness of the novel three-channel laser extensometer technique and the use of lock nuts in Kolsky tension bar experiments.

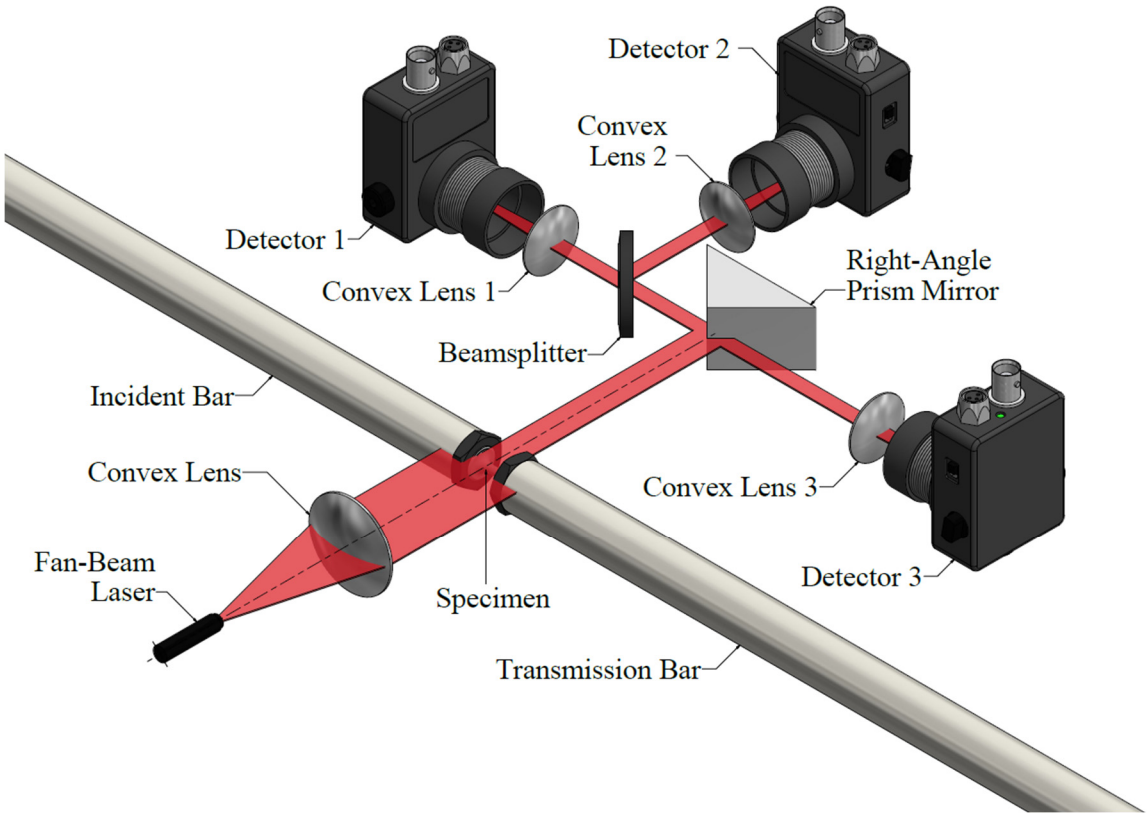

Figure 3.1: a 3D schematic of the 3-channel laser extensometer developed from the 2-channel version shown previously.

3.2. **Experimental Methods**

3.2.1. The improved Three-Channel Splitting Beam Laser Extensometer

A three-channel splitting-beam laser extensometer with hierarchical resolution was developed for the Kolsky tension bar system to directly measure the displacement of each shoulder of the tensile specimen under high strain-rate loading conditions. The configuration of this apparatus is illustrated in Figure 3.1 by a 3D schematic. A collimated sheet laser generated by an integrated line laser and convex lens is projected across the gap between the incident and transmission bar. The width of the sheet laser was precisely adjusted such that it spanned the entire gage section and transitional sections (shoulders) of the specimen. As

discussed in chapter two, a right-angle prism mirror, with its apex normal to the laser sheet, is used to split the laser beam into two independent beams in opposite directions. The beam on the Incident bar side is then split again by a pellicle beam splitter. This additional beam splitter allows the incident side beam to be measured by two different detectors with two different resolutions simultaneously. This arrangement allows one of the detectors (detector 2) to be set to a high resolution to precisely measure small deformations, however, like most measurement devices, increasing resolution results in a decrease of the overall measurement range. Therefore, the high-resolution channel will become saturated when the specimen reaches large deformations. To measure the full specimen deformation, the remaining detector (detector 1) can be tuned to have a range sufficient to measure the full specimen deformation, with slightly reduced resolution. The displacement of the transmission bar in Kolsky tension bar experiments is typically significantly smaller than the incident bar displacement. This means that the transmission bar detector (detector 3) can be set to a higher resolution, comparable to detector 2, while maintaining a sufficient measurement range. With this configuration, the high-resolution displacement signals collected by detectors 2 and 3 can be used for small elastic strain calculation which is critical for Young's modulus measurement. The lower resolution measurement obtained by detector 1 combined with the data from detector 3 are then used to calculate the large plastic deformation of the specimen. The detectors have a high-frequency bandwidth which makes them capable of measuring small displacement with a maximum resolution of approximately 500 nm. Additionally, the dual-channel configuration on the incident bar side, allows the laser extensometer to be tuned to the best compromise between measurement range and resolution, which facilitates the simultaneous measurement of specimen deformation with hierarchical resolutions.

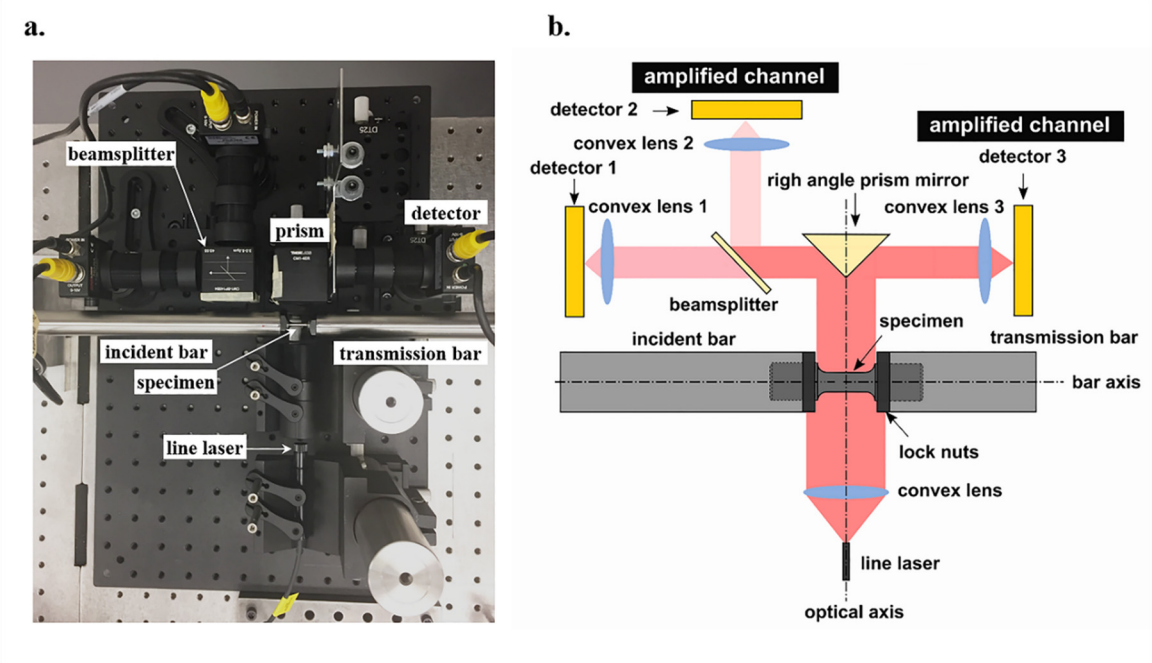

Figure 3.2: The three-channel laser extensometer developed for Kolsky tension bar experiments (a) a picture of the apparatus and (b) a schematic illustrating the manipulation of the laser beam.

Prior to dynamic tensile experiments, the sensitivity factor of the laser extensometer was carefully calibrated under static conditions by simulating the specimen displacement using a micrometer-equipped translation stage. During the calibration, the tensile specimen was not installed, and the laser beam was blocked by an opaque calibration plate rigidly attached to the translation stage. By moving the translation stage with a step size of 10 μm, the corresponding change in laser intensity can be detected by the photodetector and measured with a digital oscilloscope. Using this process, the relationship between output voltage and displacement was developed, due to the collimated laser source, this relationship is linear, with the slope being the laser sensitivity. In addition to calculating the laser sensitivity coefficients (κ_1, κ_2, and κ_3) for each detector, the calibration process is also used to verify that all the components are properly aligned. Using the calibrated sensitivity coefficients, the total tensile strain as a function of the output voltage from detectors 1 and 3 can be calculated using Equation 3.1.

$$\varepsilon_{laser-total} = \frac{\kappa_1 u_1\,(t) - \kappa_3 u_3(t)}{L_s} \tag{3.1}$$

While the elastic strain at the beginning of the specimen deformation is a function of the voltage output from channels 2 and 3 according to Equation 3.2.

$$\varepsilon_{laser-elastic} = \frac{\kappa_2 u_2\,(t) - \kappa_3 u_3(t)}{L_s} \tag{3.2}$$

Where $\boldsymbol{\kappa_1}$, $\boldsymbol{\kappa_2}$, and $\boldsymbol{\kappa_3}$ are laser sensitivity coefficients for each laser channel, while $\boldsymbol{u_1\,(t)}$, $\boldsymbol{u_2(t)}$, and $\boldsymbol{u_3(t)}$ are the laser output voltage signals for the three laser-extensometers, and $\boldsymbol{L_s}$ is the gage length of the specimen.

3.2.2. Decoupling Strain from Transitional Section

It must be noted that the displacement measured by the laser extensometer includes contributions from the gage section deformation and the deformation of the transitional sections of the specimen. The average strain over the specimen gage section is defined by Equation 3.3.

$$\varepsilon = \frac{\Delta L_s}{L_s} \tag{3.3}$$

Where ΔL_s is the total deformation of the specimen which includes the deformation of both the gage and transitional sections of the specimen. For the specimen geometry shown in Fig. 2.3, an analytical method is needed to decouple the deformation of the transitional section from the total measured specimen deformation ΔL_s in order to accurately calculate the strain of the gage section alone. When the specimen is undergoing purely elastic deformation, the elastic strain in the gage section can be calculated as a function of the total strain using a method proposed by Song et al. [1,35].

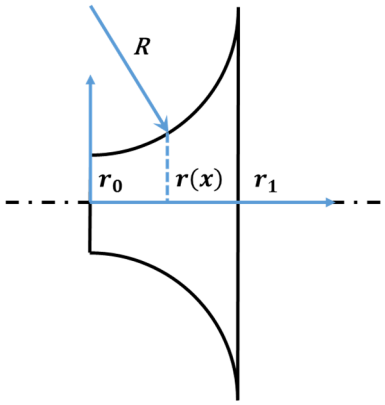

Figure 3.3: A schematic of the right-side transitional section of the prescribed specimen geometry.

Considering the specimen geometry shown in Figure 2.3 and analyzing only the geometry of the transitional section shown in Figure 3.3, the axial strain distribution in the transitional section under a certain load *F* is described by Equation 3.4.

$$\varepsilon_t(x) = \frac{F}{E_s A(x)} \tag{3.4}$$

Where E_s is the Young's modulus of the specimen material and $A(x)$ is the cross-sectional area of the specimen as a function of the axial location *x*. For the prescribed specimen geometry, the cross-sectional area as a function of the axial location is given by Equation 3.4.

$$A(x) = \pi r^2(x) \tag{3.5}$$

Where *r(x)* is the specimen radius as a function of axial location and is defined by equation 3.6.

$$r(x) = R + r_0 - \sqrt{R^2 - x^2} \tag{3.6}$$

The total deformation contributed by the transitional sections, ΔL_t, is described by equation3.7 which was found by combining Equations 3.4-3.6 and integrating over the entire transitional section, from $r(0) = r_0$ to $r(x_0) = r_1$ and multiplying by two to account for the contribution of both transitional sections.

$$\Delta L_t = 2\int_0^{x_0} \varepsilon_t dx = 2\int_0^{x_0} \frac{F}{E_s\pi\left(R + r_0 - \sqrt{R^2 - x^2}\right)^2} dx \tag{3.7}$$

For the prescribed geometry,$r_0 = 1.59mm$, $R = 3.18mm$, and $x_0 = 3.18mm$, using these constants equation 3.7 can be simplified to Equation 3.8.

$$\Delta L_t = \frac{1.538F}{E_s\pi} \text{ (mm)} \tag{3.8}$$

When the load *F* is relatively low and the entire specimen is still undergoing purely elastic deformation, the deformation of the gage section is described by Equation 3.9.

$$\Delta L_g = \frac{F}{E_s\pi} \cdot \frac{L_s}{r_0^2} = \frac{2.512F}{E_s\pi} \text{ (mm)} \tag{3.9}$$

More details of this derivation process can be found in Refs. [1,35]. Using Equations 3.8 and 3.9, the contribution of the strain in the gage section to the total deformation measured by the laser-extensometer can be calculated as follows.

$$C' = \frac{\Delta L_g}{\Delta L_g + \Delta L_t} = 0.62 \tag{3.10}$$

Equation 3.10 shows that 62% of the total elastic deformation measured by the laser extensometer is a result of the deformation in the gage section of the specimen. This procedure assumes that the entire specimen is under uniaxial tension, while in reality there are likely more complex stress states present especially in the specimen shoulders. However, this procedure gives a good zero order approximation of the deformation and

the results show good agreement with experimental measurements. The Young's Modulus of the specimen gage section can then be calculated according to Equation 3.11.

$$E_s = \frac{\sigma}{0.62\ \varepsilon_{laser-elastic}} \tag{3.11}$$

Where $\boldsymbol{\sigma}$ is the applied stress, which is calculated using the transmitted wave and the conventional Kolsky bar equations, according to Equation 3.12.

$$\sigma = \frac{F}{A_s} = \frac{A_B E_B \varepsilon_T}{A_s} \tag{3.12}$$

Where $\boldsymbol{E_b}$ is the Young's modulus of the bar material. $\boldsymbol{A_b}$ and $\boldsymbol{A_s}$ are the cross-sectional areas of the bar and specimen gage section, respectively.

As mentioned above, the correction factor C' is only applicable when the specimen is undergoing purely elastic deformation. Once the gage section surpasses its yield stress and plastic deformation begins, the deformation in the transitional sections of the specimen will remain elastic due to the significantly larger cross-sectional area. If the specimen-material response is perfectly plastic, or the work hardening is negligible, then the applied force will not increase significantly as the gage section undergoes plastic deformation. Therefore, the deformation in the transitional section will remain elastic [35] and the calculation of the transitional section deformation using Equation 3.7 will remain valid. As long as the deformation in the transitional region remains elastic, the deformation of the gage section can be calculated using Equation 3.13, using the applied force calculated in Equation 3.12 and the Young's Modulus from Equation 3.11.

$$\Delta L_g = \Delta L_{total} - \Delta L_t \tag{3.13}$$

As mentioned previously, the total displacement, ΔL_{total}, is calculated according to Equation 3.14 using the reflected wave, $\boldsymbol{\varepsilon_r(t)}$, recorded by the strain gages on the incident bar.

$$\Delta L_{total} = -2C_b \int_0^t \varepsilon_r(t)dt \tag{3.14}$$

Where C_b is the elastic wave speed in the bars. But due to the complex interfaces between the bar ends and the tensile specimen, the reflected pulse may not be an accurate method of calculating the total displacement. In this study, the total displacement, ΔL_{total}, is directly measured using the laser extensometer. Furthermore, the direct displacement measurement with the new laser extensometer can also be used to assess the uncertainties of specimen displacement calculation with the reflected pulse and the effectiveness of the lock nuts applied to the tensile specimen with different levels of torque.

3.3. **Results and Discussion**

3.3.1. Laser Extensometer Calibration

The correlation between bar displacement and laser detector signal output must be carefully calibrated prior to conducting dynamic tension experiments. This calibration procedure provides sensitivity coefficients, for all three laser channels (κ_1, κ_2, and κ_3), that represent the slope of the linear relationship between displacement and detector output voltage. The calibration procedure allows the specimen deformation during a dynamic test to be calculated using Equations 3.1 and 3.2. The calibration procedure was conducted using a high-resolution differential translation stage equipped with a micrometer for precise movement, a schematic of the calibration device is shown in Figure 3.4. As shown, a metal plate is affixed to the translation stage, such that it blocks a portion of the laser beam in place of one of the bars, therefore the gap through which the beam passes is defined by the plate and the opposite bar end. Moving the translation stage simulates the motion of the bar end, changing the gap width, which results in a corresponding change in the amount of light reaching the detector and therefore the detector's voltage output. This arrangement allows the voltage output of the detector to be calibrated against the known displacement of the high-resolution translation stage.

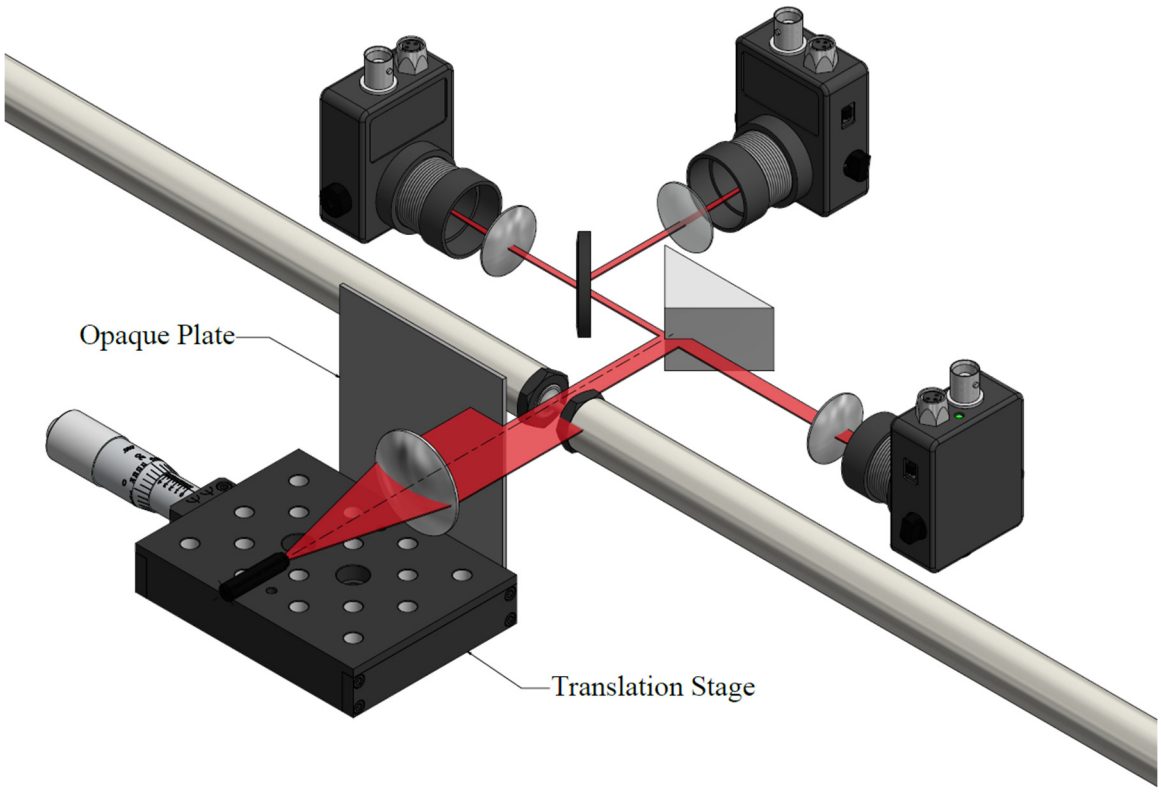

Figure 3.4 A Schematic of the laser extensometer calibration system

With this calibration method, the sensitivity for each individual laser channel can be calculated, the resulting correlations between displacement and voltage output are shown in Fig. 3.5. It should be noted that each channel was calibrated over a displacement range expected for that channel during a typical Kolsky bar experiment. As shown in Figure 3.5, the relationship between displacement and output voltage is nearly perfectly linear for all three channels. Therefore, the bar displacement as a function of voltage output for each channel can be characterized by a single scalar constant, the sensitivity coefficient (κ_1, κ_2, or κ_3), which is simply the slope of the voltage versus displacement plot.

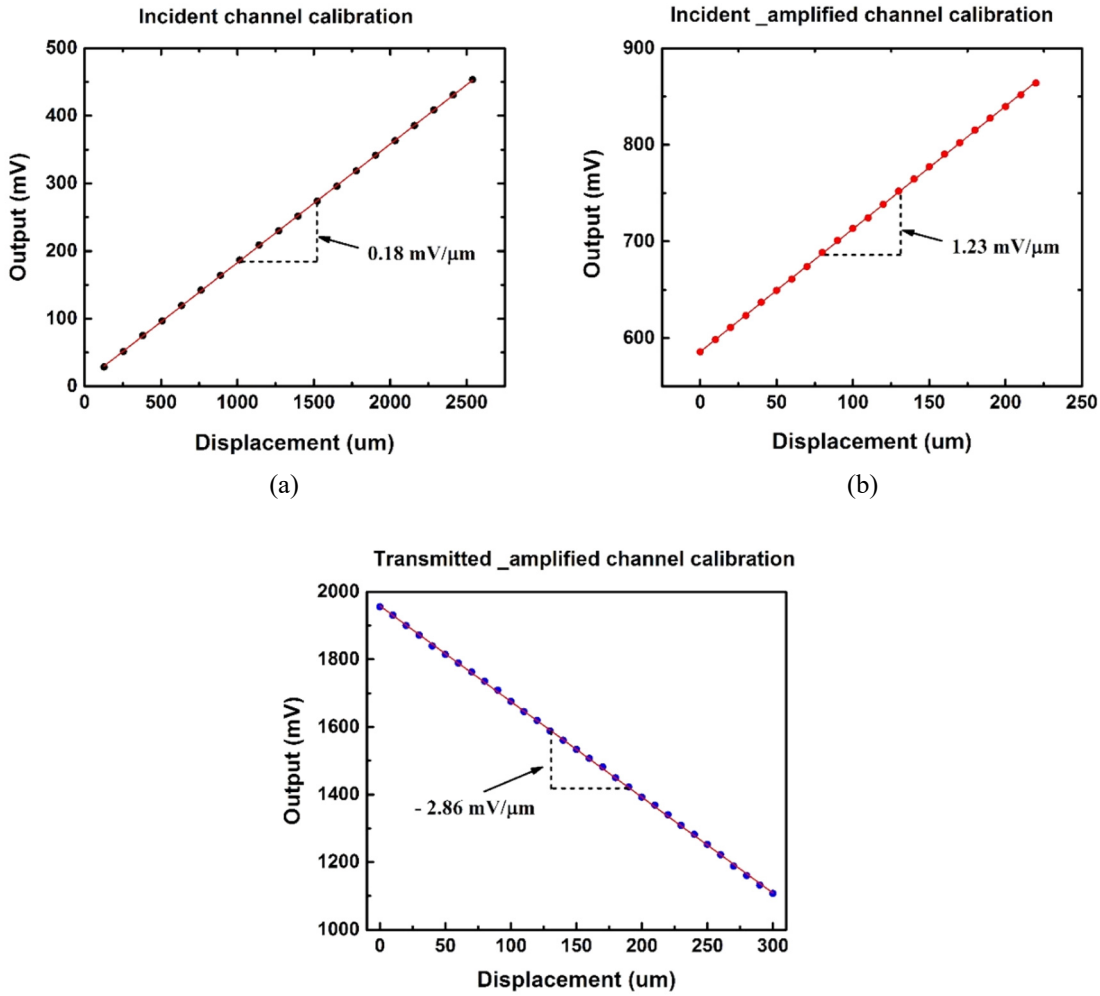

Figure 3.5: Calibration results for the three laser channels, (a) the full range (unamplified) Incident bar channel, (b) the high-resolution (amplified) Incident bar channel, and (c) the high-resolution transmission bar channel

Figures 3.5b and 3.5c also illustrate the significant difference in the sensitivity magnitude between the two amplified channels despite the identical amplification used in both cases. This discrepancy is caused by the change in the laser intensity across the entire specimen length, further emphasizing the need for the splitting beam laser extensometer configuration. The sensitivity coefficients obtained from the calibration procedure are summarized in table 3.1. The final spatial resolution is dependent on the sensitivity of the instrument used to measure the laser detector output, the resulting spatial resolutions assuming a measurement sensitivity of 1mV are listed in table 3.1 as well.

Table 3.1: Calibration Parameters for the three laser channels.

	Incident	Incident Amplified	Transmitted Amplified
Estimated Displacement	1.9 mm	100 μm	160 μm
Calibration Range	0 - 2.5 mm	0 - 200 μm	0 - 300 μm
Calibration step size	0.127 mm	10 μm	10 μm
Sensitivity Coefficient	0.18 mV/μm	1.23 mV/μm	-2.86 mV/μm
Maximum Resolution	5.5 μm	813 nm	350 nm

3.3.2. Effect of Locknuts

In this study, the testing conditions were kept the same for all dynamic tensile experiments on the same material, 304L stainless steel, at the same strain rate of 670 s^{-1}. A set of signals from a typical test, as recorded by the oscilloscope are shown in Figure 3.6, it must be noted that the signals from detectors 2 and 3 are amplified 31.6 times for clarity. The plateau that appears on the reflected pulse indicates that the specimen was deformed at a constant strain rate. Also note that while detectors 1 and 2 are both measuring the same displacement, detector 2 becomes saturated after 340 μs. As mentioned previously, the use of lock nuts is expected to improve the thread engagement at the bar/specimen interface which may improve the accuracy of displacement calculations using the wave mechanics equations.

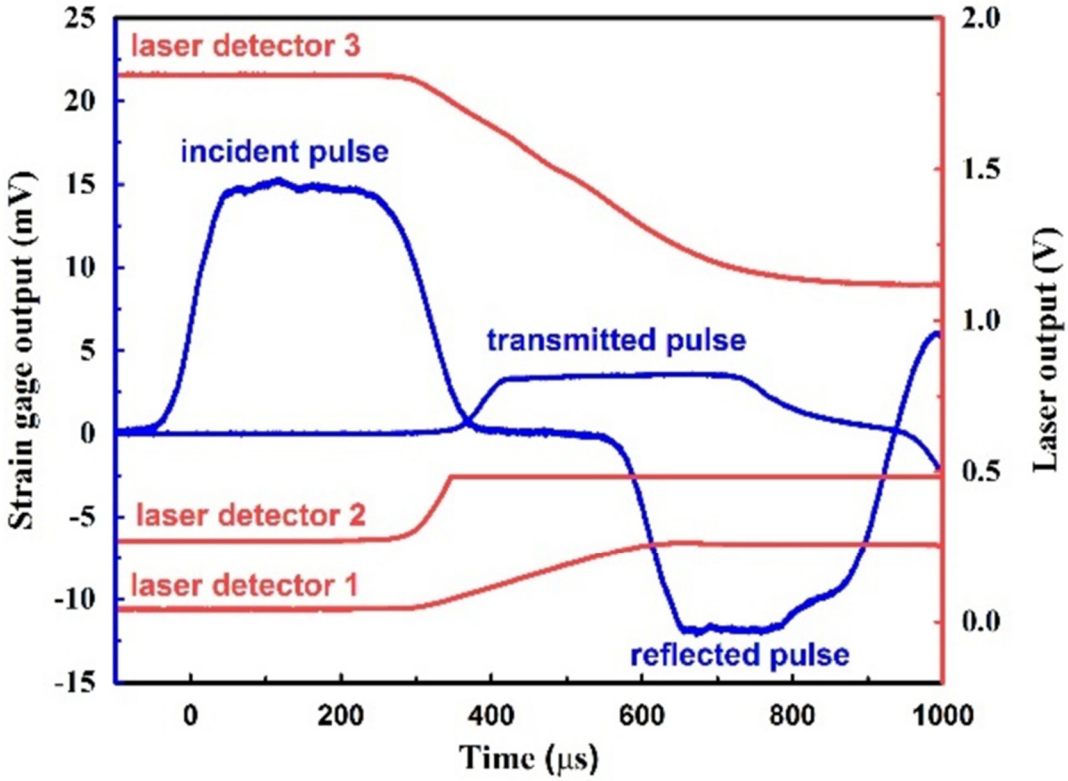

Figure 3.6: Oscilloscope signals from the three laser detectors and two strain gages obtained during a typical Kolsky tension bar test.

The Displacement of Incident and Transmission bar ends are calculated using Equations 3.15 and 3.16 respectively.

$$\delta_I = C_b \int_0^t \big(\varepsilon_i(t) - \varepsilon_r(t)\big)dt \tag{3.15}$$

$$\delta_T = C_b \int_0^t \varepsilon_t(t)dt \tag{3.16}$$

Where δ_I and δ_T represent the displacement of the incident and transmission bar ends as a function of time, respectively. $\boldsymbol{\varepsilon_i(t)}$, $\boldsymbol{\varepsilon_r(t)}$, and $\boldsymbol{\varepsilon_t(t)}$ are the incident, reflected, and transmitted strain waves, respectively. The Displacements measured with the laser extensometer were then compared with the displacements

calculated using Equations 3.15 and 3.16, these results are shown in Figure 3.7. The dynamic tensile experiments used for this comparison were conducted on 304L stainless steel specimens, with three different testing conditions: without lock nuts (specimens hand tightened to the bar), with lock nuts tightened to 7.8 N·m, and with lock nuts tightened to 15.6 N·m. Figures 3.7 (a) and 3.7 (b) show a comparison of the two displacements measured at each bar end when lock nuts are not applied. Without lock nuts, the displacement of the Incident bar end calculated with the strain gage signals appears to deviate from the laser extensometer measurement beginning at about 182 μs. While the calculated displacement of the transmission bar end lags behind the laser extensometer measurement by approximately 16 μs throughout the entire deformation. These discrepancies are likely caused by the time required for the threaded interfaces to become fully engaged, because the specimens were only hand tightened into the bar ends. This engagement process resulted in a relatively higher particle velocity at the specimen shoulder on the incident bar side which caused the deviation shown in figure 3.7(a) and the delay in the transmitted wave shown in figure 3.7(b). While the displacement measured using the reflected wave is disrupted by the poor threaded connection, the laser extensometer technique remains unaffected as it measures displacement directly. However, the strain measurement obtained using the reflected wave can be improved through the application of locknuts, as shown in Figures 3.7(c-f) which show a decrease in the discrepancy between the two measurement techniques as the lock nut torque is increased. As shown in Figure 3.7(f), at the maximum torque of 15.6 N·m, the displacement at the sample shoulder on the transmission bar side is around 220 μm and the displacement histories obtained by both techniques are in close agreement.

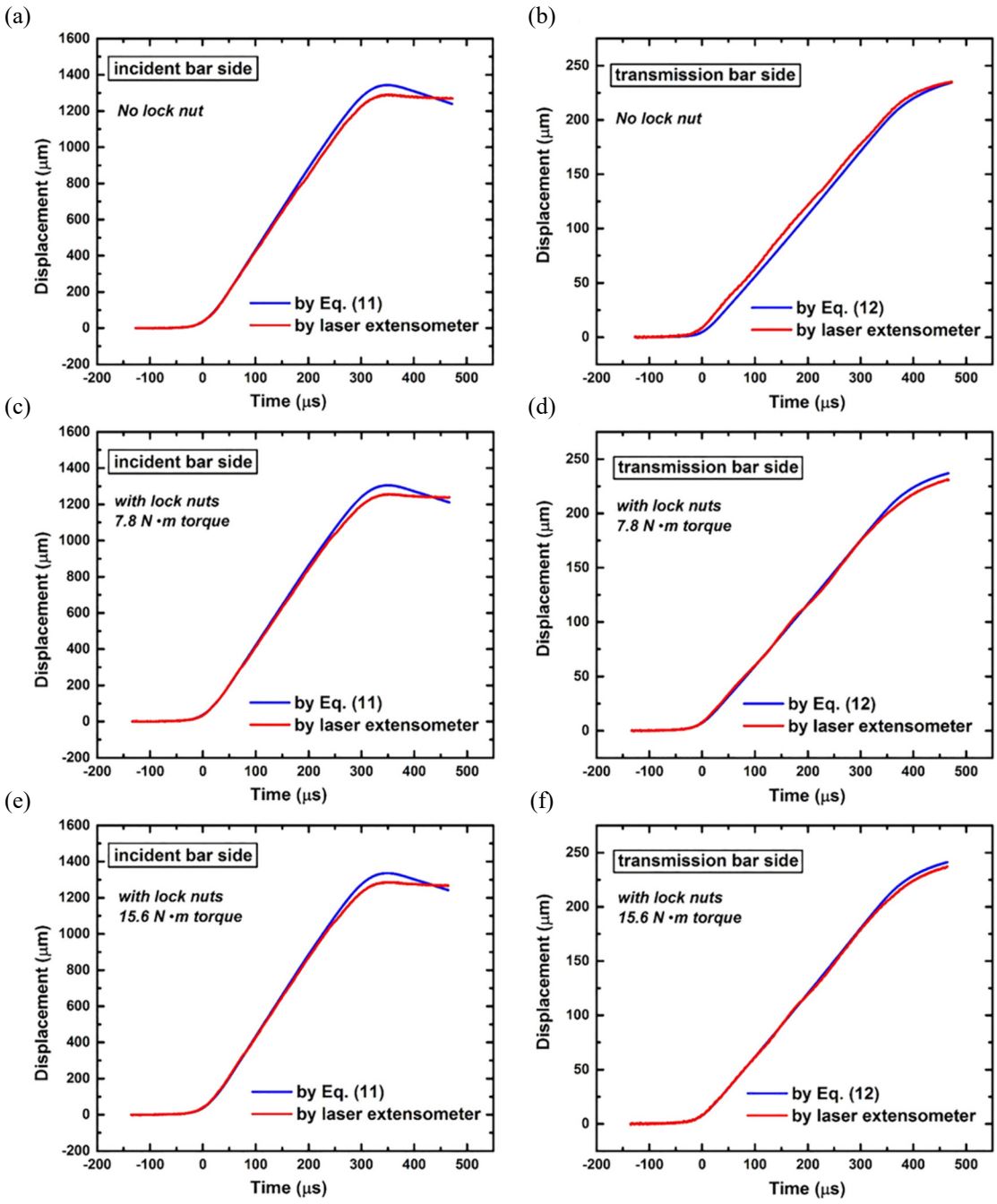

Figure 3.7: Comparison of specimen shoulder displacement measurement techniques at both the incident and transmission bar sides, with no lock nuts (a)(b), with lock nuts tightened to 7.8 N·m (c)(d), and with lock nuts tightened to 15.6 N·m (e)(f).

3.3.3. Strain Measurement with Dual Resolution

The dynamic tensile stress-strain curves of 304L stainless steel specimens tested under three different conditions (without lock nuts, with lock nuts tightened to 7.8 N·m, and with lock nuts tightened to 15.6 N·m) were calculated and corrected using the method described in equations 3.1 – 3.14, and the results are shown in Figure 6. Clearly, the discrepancy in the measurement of the specimen elastic deformation between the two techniques is highly dependent on the application of locknuts. Without the lock nuts, there is an apparent discrepancy between the two stress-strain curves at small strains, shown in Figure 3.8 (a), where the reflected wave signal yielded slightly larger strain measurements resulting in a lower apparent Young's modulus. The application of lock nuts with increasing levels of torque improves the agreement between the stress-strain curves obtained using the two techniques. With lock nuts applied and tightened to 15.6 N·m the two stress strain curves are in near perfect agreement. These results show that the thread engagement at the bar/specimen interface has a significant influence on the results obtained from Kolsky tension bar experiments and that the application of lock nuts, tightened to the appropriate torque level, improves the accuracy of these results.

Unlike the previous splitting beam laser extensometer technique, where one sub-laser beam was used to track the displacement of each specimen shoulder [46], the improved technique used in this study utilized an additional high-resolution laser channel to independently and precisely track the small deformation of the specimen. As shown in Figure 3.8 a linear regression was performed on the elastic portion of the stress-strain curves obtained using the laser extensometer to calculate the Young's modulus of the specimen. From the three testing conditions, the calculated young's modulus ranged from 195.3 GPa to 203.0 GPa. This result agrees well with the Young's modulus for this material measured in quasi-static tests, which usually ranges between 193 and 200 GPa. The consistency of the laser extensometer results indicate that this technique is not affected by either the discontinuity in the Kolsky tension bar or the gripping issues of the tensile specimen.

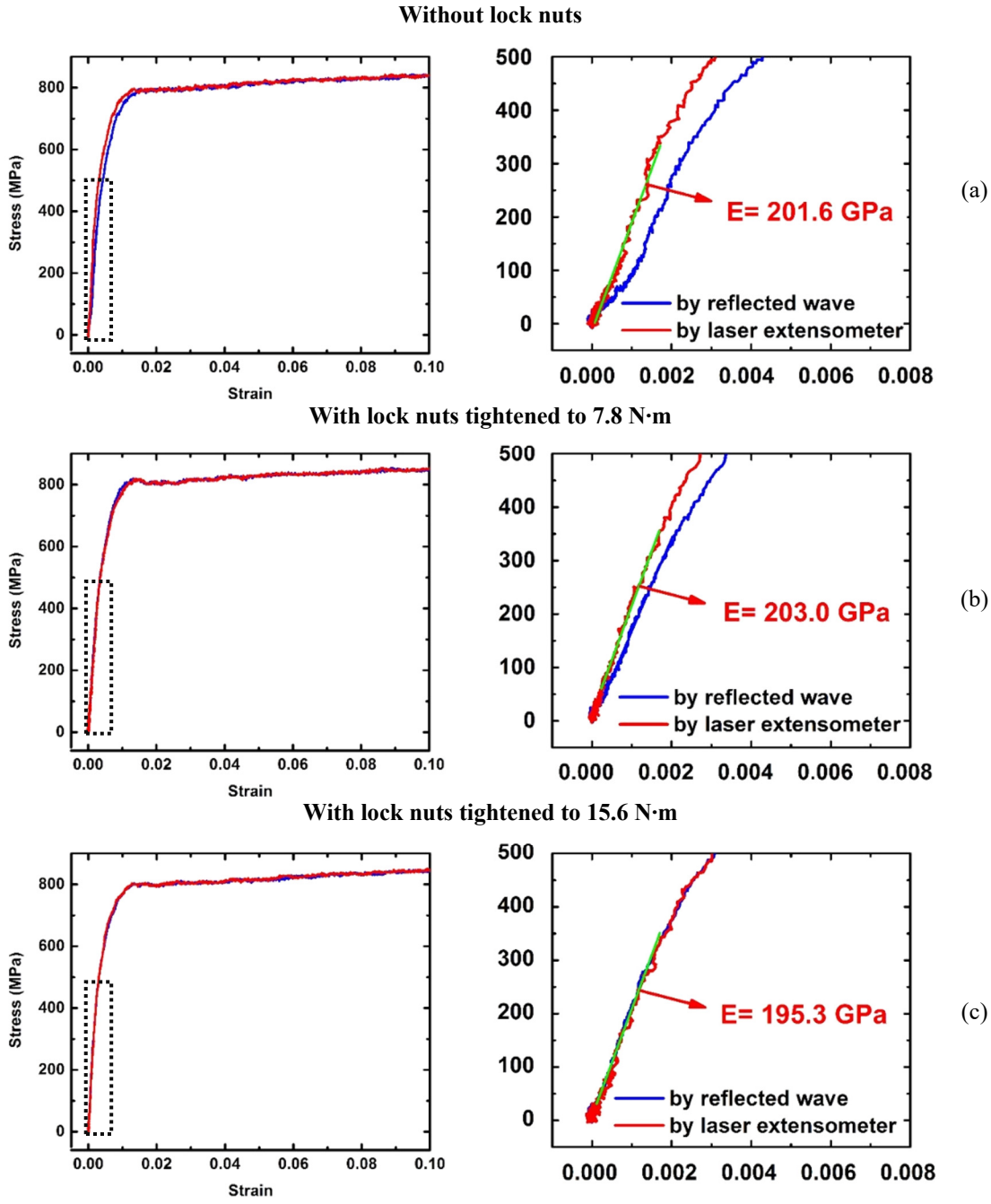

Figure 3.8: Comparison of the dynamic tensile stress-strain curves obtained using the wave mechanics equations and direct laser-extensometer measurement with three different testing conditions (a) without lock nuts, (b) with lock nuts tightened to 7.8 N·m, and (c) with lock nuts tightened to 15.6 N·m. The inset plots on the right show the elastic portion of the deformation outlined by the dotted line.

3.4. **Conclusion**

An improved three-channel splitting-beam laser extensometer technique was developed to improve the accuracy and precision of specimen deformation measurement in Kolsky tension bar experiments. While this technique does not offer the full field strain measurement provided by other techniques such as DIC, it does offer a relatively simple, and inexpensive method to accurately measure specimen deformation in dynamic experiments. This improved laser extensometer can also be implemented to other dynamic or quasi-static experimental apparatus for precise displacement measurements. This new technique employed two independent laser channels with different resolutions to track the displacement of the specimen shoulder on the incident bar side in addition to a high resolution channel on the transmission bar side. This hierarchical resolution facilitates precise deformation measurement at both small and large strains. The efficacy of this technique was demonstrated with dynamic tensile tests of 304L stainless steel specimens using a modified Kolsky tension bar at the strain rate of 670 s^{-1}. The resultant tensile stress-strain curves obtained using the laser extensometer measurements exhibited a calculated Young's moduli with a reasonable variation between 195.3 GPa to 203.0 GPa under all three testing conditions, these results agree well with the quasi-static Young's modulus of this material which is usually between 193 and 200 GPa.

Using the new three-channel splitting-beam laser extensometer technique, the effect of lock nuts employed to enhance the thread connection at the bar/specimen interface was thoroughly examined. It was shown that without lock nuts, the stress-strain curve obtained using the reflected wave resulted in a lower calculated Young's modulus than when calculated using the laser-extensometer data. This is mainly due to the poor thread engagement at the bar/specimen interface disrupting the reflected wave. When lock nuts were applied and tightened to 15.6 N·m, the stress-strain curve calculated with the reflected wave became nearly identical to that calculated with the laser extensometer signals at both small and large strains. Based on this evidence, it is believed that lock nuts are an essential modification to the Kolsky tension bar testing of metallic specimens to improve thread engagement at the specimen/bar interface and thereby improve the accuracy of specimen deformation measurement. As shown, when lock nuts are used and tightened to the appropriate torque, the accuracy of strain calculation using the reflected wave becomes comparable to direct measurement using the laser extensometer technique.

Chapter 4

SUMMARY AND FUTURE WORK

4.1. **Summary**

Strain measurement in Kolsky tension bar experiments has long been a challenging topic due to complexities in specimen/bar engagement as well as non-standard specimen geometries. The challenges associated with specimen gripping, geometric discontinuities, thread tolerances, and the relatively short uniform gage section all compromise the accuracy of the conventional strain calculation technique based on one dimensional stress wave theory. Local techniques using strain gages often provide limited measurement range, while full-field techniques such as DIC do not offer sufficient resolution at very small strains. The conventional laser occlusive extensometer technique provides an alternative to the one-dimensional stress wave-based strain measurement method that is insensitive to the effects of thread engagement. However, this technique is based on the assumption that the laser intensity along the specimen gage section remains constant, which is typically not a valid assumption for most laser systems. This deviation in laser intensity coupled with rigid body motion of the specimen results in false deformation measurement and introduces significant uncertainties to the strain calculation

To account for the influence of a non-uniform laser intensity, a modified laser occlusive extensometer technique was developed to measure the specimen strain with reasonably high and tunable resolutions for use in Kolsky tension bar experiments. This technique provides the precision required for small strain measurement, without sacrificing the measurement range required for large plastic deformations. This technique also minimizes the uncertainty caused by rigid body motion of the specimen coupled with non-uniform laser intensity across the gage length. The validation test on Vascomax® maraging C250 alloy demonstrated that the new technique was capable of measuring both small and large strains in Kolsky tension bar experiments, this technique is also applicable to Kolsky compression bar experiments.

Expanding on the novel concept of splitting the laser beam to measure the displacements of the incident and transmission bars independently, a further improvement was implemented to allow dual-channel measurement on the incident bar side. This modification allowed the incident bar displacement to be measured with two different resolutions, the higher resolution channel is used to measure the small elastic deformation, while the lower resolution channel used to measure large plastic deformations. Through careful instrumentation and calibration of the three laser channels, the resolution and measurement range of each channel were coordinated to provide precise measurement at both small and large strains under high strain-rate tensile loading conditions. This novel design facilitates a maximum displacement measurement resolution of approximately 500 nm, which corresponds to a strain resolution of 0.0079% for a specimen with a 6.35-mm gage length. To further improve the accuracy of strain measurement, a pair of locknuts were used to improve the connection between the specimen and bars. Tightening the locknuts to an appropriate torque level improves thread engagement at the specimen /bar interface in addition to preventing potential pre-torsional deformation and damage during installation. Results from dynamic tensile experiments conducted on 304L stainless steel specimens demonstrated that the application of locknuts tightened to the proper torque level, improved the accuracy of small strain measurement significantly. To address the contribution of elastic deformation in the transitional section of the specimen to the total measured deformation, an analytical strain correction procedure was adopted. The three-channel laser extensometer technique has proven to be an effective and accurate alternative for strain measurement under high strain-rate tensile deformation.

4.2. **Future Work**

The effectiveness of the splitting-beam laser extensometer technique has been demonstrated through comparison with the conventional strain gage technique. Additionally, the implementation of locknuts was shown to significantly improve the results obtained using the conventional strain measurement technique. As both methods measure the total deformation of the gage section, no local deformations can be measured using either technique. The use of a full field measurement technique, such as DIC, in conjunction with the laser extensometer could be used to investigate the local deformation in the gage section. Additionally, DIC could be used to measure the global deformation for comparison with the laser extensometer measurements

for further validation of this novel technique. However, due to its lower resolution, DIC is in capable of resolving the small elastic strains, therefore only the large plastic strain measurement could be compared with the laser extensometer data.

The strain correction procedure used in this study was developed with the assumption that the transitional section of the specimen undergoes purely elastic deformation throughout the loading process. This assumption is valid if the specimen material exhibits a nearly perfectly plastic response so that the strain hardening effects are negligible and the stress does not increase significantly throughout the plastic deformation process. For metallic materials that exhibit significant strain hardening, this correction procedure will not account for plastic deformation that occurs in the transitional section of the specimen, and therefore over estimate the total strain in the gage section. This error may become significant for materials with large strain hardening rate and will need to be addressed in a future effort while developing an improved strain correction method.

4.3. **Related Publications**

Xu Nie, Bo Song, Colin Loeffler, "A Novel Splitting-Beam Laser Extensometer Technique for Kolsky Tension Bar Experiment", Journal of Dynamic Behavior of Materials, 2015, Vol. 1, 70-74

Ying Qiu, Colin Loeffler, Xu Nie, Bo Song, "Improved Experimental and Diagnostic Techniques for Dynamic Tensile Stress-Strain Measurement With A Kolsky Tension Bar", Measurement Science and Technology, 2018 (accepted)

REFERENCES

[1] Song B, Antoun B R and Jin H 2013 Dynamic Tensile Characterization of a 4330-V Steel with Kolsky Bar Techniques *Exp. Mech.* **53** 1519–29

[2] TAYLOR G I 1946 JAMES FORREST LECTURE 1946. THE TESTING OF MATERIALS AT HIGH RATES OF LOADING. *J. Inst. Civ. Eng.* **26** 486–519

[3] Walley S and Eakins D 2014 Introduction *Philos. Trans. R. Soc. A Math. Phys. Eng. Sci.* **372** 20130220–20130220

[4] Kolsky H 1949 An Investigation of the Mechanical Properties of Materials at very High Rates of Loading *Proc. Phys. Soc. Sect. B* **62** 676–700

[5] Chen W W, Wu Q, Kang J H and Winfree N A 2001 Compressive superelastic behavior of a NiTi shape memory alloy at strain rates of 0.001–750 s−1 *Int. J. Solids Struct.* **38** 8989–98

[6] Smerd R, Winkler S, Salisbury C, Worswick M, Lloyd D and Finn M 2005 High strain rate tensile testing of automotive aluminum alloy sheet *Int. J. Impact Eng.* **32** 541–60

[7] Dixit N, Xie K Y, Hemker K J and Ramesh K T 2015 Microstructural evolution of pure magnesium under high strain rate loading *Acta Mater.* **87** 56–67

[8] Song B, Nelson K, Lipinski R, Bignell J, Ulrich G B and George E P 2015 Dynamic High-Temperature Tensile Characterization of an Iridium Alloy with Kolsky Tension Bar Techniques *J. Dyn. Behav. Mater.* **1** 290–8

[9] Lankford J 1981 Mechanisms Responsible for Strain-Rate-Dependent Compressive Strength in Ceramic Materials *J. Am. Ceram. Soc.* **64** C-33-C-34

[10] Jiao T, Li Y, Ramesh K T and Wereszczat A A 2005 High Rate Response and Dynamic Failure of Structural Ceramics *Int. J. Appl. Ceram. Technol.* **1** 243–53

[11] Chen W W, Rajendran A M, Song B and Nie X 2007 Dynamic fracture of ceramics in armor applications *J. Am. Ceram. Soc.* **90** 1005–18

[12] Grote D L, Park S W and Zhou M 2001 Dynamic behavior of concrete at high strain rates and pressures: I. experimental characterization *Int. J. Impact Eng.* **25** 869–86

[13] Riisgaard B, Ngo T, Mendis P, Georgakis C T and Stang H 2007 Dynamic increase factors for high performance concrete in compression using split hopkinson pressure Bar *6th Int. Conf. Fract. Mech. Concr. Concr. Struct.*

[14] Xiao J, Li L, Shen L and Poon C S 2015 Compressive behaviour of recycled aggregate concrete under impact loading *Cem. Concr. Res.* **71** 46–55

[15] Song B, Chen W W, Dou S, Winfree N A and Kang J H 2005 Strain-rate effects on elastic and early cell-collapse responses of a polystyrene foam *Int. J. Impact Eng.* **31** 509–21

[16] Kendall M J, Froud R F and Siviour C R 2014 Novel temperature measurement method & thermodynamic investigations of amorphous polymers during high rate deformation *Polymer (Guildf).* **55** 2514–22

[17] Fan J T, Weerheijm J and Sluys L J 2015 High-strain-rate tensile mechanical response of a polyurethane elastomeric material *Polymer (Guildf).* **65** 72–80

[18] Nie X, Cheng J-I, Chen W W and Weerasooriya T 2011 Dynamic Tensile Response of Porcine Muscle *J. Appl. Mech.* **78** 021009

[19] Lim J, Hong J, Chen W W and Weerasooriya T 2011 Mechanical response of pig skin under dynamic tensile loading *Int. J. Impact Eng.* **38** 130–5

[20] Saraf H, Ramesh K T, Lennon A M, Merkle A C and Roberts J C 2007 Mechanical properties of soft human tissues under dynamic loading *J. Biomech.* **40** 1960–7

[21] Chen W and Song B 2011 *Split Hopkinson (Kolsky) Bar* (Boston, MA: Springer US)

[22] Chiddister J L and Malvern L E 1963 Compression-impact testing of aluminum at elevated

temperatures *Exp. Mech.* **3** 81–90
[23] Song B, Antoun B R, Connelly K, Korellis J and Lu W-Y 2011 Improved Kolsky tension bar for high-rate tensile characterization of materials *Meas. Sci. Technol.* **22** 045704
[24] Owens A T and Tippur H V 2009 A Tensile Split Hopkinson Bar for Testing Particulate Polymer Composites Under Elevated Rates of Loading *Exp. Mech.* **49** 799–811
[25] Chen W, Lu F, Frew D J and Forrestal M J 2002 Dynamic Compression Testing of Soft Materials *J. Appl. Mech.* **69** 214
[26] Gorham D A 1989 Specimen inertia in high strain-rate compression *J. Phys. D. Appl. Phys.* **22** 1888–93
[27] Lindholm U S and Yeakley L M 1968 High strain-rate testing: Tension and compression *Exp. Mech.* **8** 1–9
[28] Harding J, Wood E 0 and Campbell J D 1960 Tensile testing of materials at impact rates of strain *J. Mech. Eng. Sci.* **2** 88–96
[29] Hauser F E 1966 Techniques for measuring stress-strain relations at high strain rates *Exp. Mech.* **6** 395–402
[30] Harding J and Welsh L M 1983 A tensile testing technique for fibre-reinforced composites at impact rates of strain *J. Mater. Sci.* **18** 1810–26
[31] Nicholas T 1981 Tensile testing of materials at high rates of strain *Exp. Mech.* **21** 177–85
[32] Staab G H and Gilat A 1991 A direct-tension split Hopkinson bar for high strain-rate testing *Exp. Mech.* **31** 232–5
[33] Heard W F, Martin B E, Nie X, Slawson T and Basu P K 2014 Annular Pulse Shaping Technique for Large-Diameter Kolsky Bar Experiments on Concrete *Exp. Mech.* **54** 1343–54
[34] Guzman O, Frew D J and Chen W 2011 A Kolsky tension bar technique using a hollow incident tube *Meas. Sci. Technol.* **22** 045703
[35] Song B, Wakeland P E and Furnish M 2015 Dynamic Tensile Characterization of Vascomax® Maraging C250 and C300 Alloys *J. Dyn. Behav. Mater.* **1** 153–61
[36] Li M, Wang R and Han M-B 1993 A Kolsky bar: Tension, tension-tension *Exp. Mech.* **33** 7–14
[37] Nguyen K-H, Kim H C, Shin H, Yoo Y-H and Kim J-B 2017 Numerical investigation into the stress wave transmitting characteristics of threads in the split Hopkinson tensile bar test *Int. J. Impact Eng.* **109** 253–63
[38] Moore K J, Kurt M, Eriten M, Dodson J C, Foley J R, Wolfson J C, McFarland D M, Bergman L A and Vakakis A F 2017 Nonlinear Parameter Identification of a Mechanical Interface Based on Primary Wave Scattering *Exp. Mech.* **57** 1495–508
[39] Smith B W, Li X and Tong W 1998 Error assessment for strain mapping by digital image correlation *Exp. Tech.*
[40] Hoult N A, Andy Take W, Lee C and Dutton M 2013 Experimental accuracy of two dimensional strain measurements using Digital Image Correlation *Eng. Struct.* **46** 718–26
[41] Pan B, Yu L, Wu D and Tang L 2013 Systematic errors in two-dimensional digital image correlation due to lens distortion *Opt. Lasers Eng.* **51** 140–7
[42] Grédiac M, Sur F and Blaysat B 2016 The Grid Method for In-plane Displacement and Strain Measurement: A Review and Analysis *Strain* **52** 205–43
[43] Zhu D, Mobasher B and Rajan S D 2012 Non-contacting strain measurement for cement-based composites in dynamic tensile testing *Cem. Concr. Compos.* **34** 147–55
[44] Zhu D, Mobasher B and Rajan S D 2011 Non-contacting strain measurement in Dynamic Tensile Testing *Experimental and Applied Mechanics* vol 6, ed T Proulx (Springer) pp 209–16
[45] Li Y and Ramesh K T 2007 An optical technique for measurement of material properties in the tension Kolsky bar *Int. J. Impact Eng.* **34** 784–98
[46] Nie X, Song B and Loeffler C M 2015 A Novel Splitting-Beam Laser Extensometer Technique for Kolsky Tension Bar Experiment *J. Dyn. Behav. Mater.* **1** 70–4
[47] Joyce B S, Dennis M, Dodson J and Wolfson J 2017 Characterization of a Laser Extensometer for Split Hopkinson Pressure bar Experiments *Exp. Mech.* **57** 1265–73
[48] Panowicz R, Janiszewski J and Traczyk M 2017 Strain measuring accuracy with splitting-beam laser extensometer technique at split Hopkinson compression bar experiment *Bull. Polish Acad. Sci. Tech. Sci.* **65** 163–9
[49] Ramesh K T and Narasimhan S 1996 Finite deformations and the dynamic measurement of radial

strains in compression Kolsky bar experiments *Int. J. Solids Struct.* **33** 3723–38
[50] Ostwaldt D, Klepaczko J R and Klimanek P 1997 Compression Tests of Polycrystalline α-Iron up to High Strains Over a Large Range of Strain Rates *Le J. Phys. IV* **07** C3-385-C3-390
[51] Lim J, Chen W W and Zheng J Q 2010 Dynamic small strain measurements of Kevlar® 129 single fibers with a miniaturized tension Kolsky bar *Polym. Test.* **29** 701–5
[52] Hudspeth M, Nie X, Chen W and Lewis R 2012 Effect of Loading Rate on Mechanical Properties and Fracture Morphology of Spider Silk *Biomacromolecules* **13** 2240–6